



国家海洋环境预报中心
NATIONAL MARINE ENVIRONMENTAL FORECASTING CENTER
国家海洋预报台



Preliminary Study of MLD and SCML in the SCS using 3-D physical-biogeochemical model



Guimei Liu, Xuanliang Ji

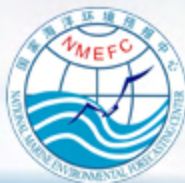
National Marine Environmental Forecasting Center,

Beijing, China

November 23, 2018

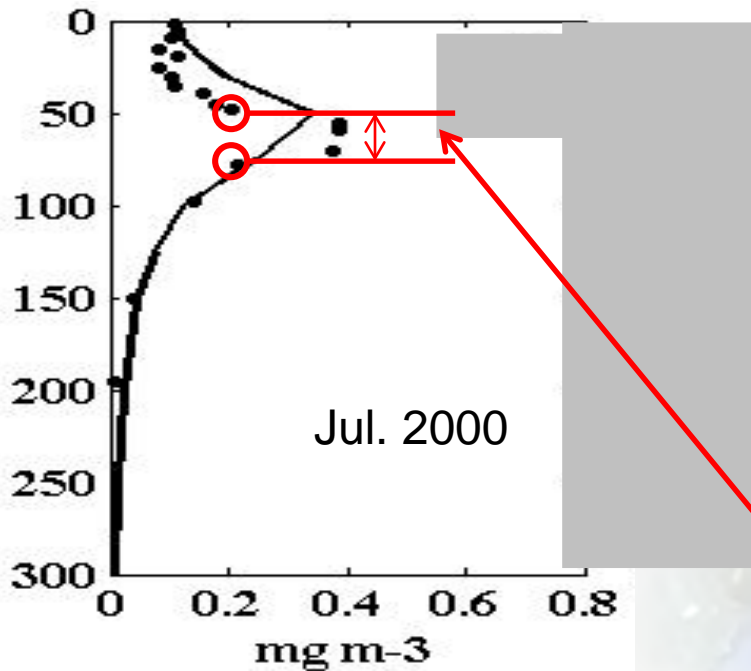
Outline

- Brief Introduction
- Model Configuration
- Model results and Discussion
- Conclusion



Brief Introduction

- **SCML:** Subsurface Chlorophyll Maximum Layer, including three characterization factors which are Depth, Strength and thickness.
- Beckmann and Hense (2007) defines these three characterization factors from the dynamic aspect.

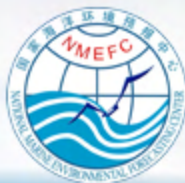


Depth: the water depth of the maximum chlorophyll concentration occurring at, which is also the maximum biomass of zooplankton at. Hence, the factor of depth could provide information of fishery;

Strength: the maximum concentration of subsurface chlorophyll, or the vertical integration value at SCML. Beckmann and Hense (2007) thought it's more reasonable using the integration value to study the SCML.

Thickness: the range of SCML. Simplest definition: the range between the two positions located at the two sides of SCML with the same concentration value (or a constant percentage of SCM, like 50%)

Example: Chlorophyll-a at SEAST



| Position | | Longitude and Latitude | Thickness (m) | Strength (mg/m ³) | Depth (m) | Reference | | |
|---|---------------------------------------|-------------------------|--|-------------------------------|---------------|-----------------------------|--------------------------|--------------------------|
| Ocean | Tropic Sub-tropic | West Pacific | 17-20°S 165°E | --- | 0.25-0.3 | 80-110 | Radenac and Rodier, 1996 | |
| | | | 6-10°N 165°E | --- | 0.15-0.25 | 80-120 | | |
| | | The South China Sea | 12-19.5°N 111-118°E | --- | 0.1-0.6 | 50-100 | Chen et al., 1989 | |
| | | | ALOHA Station at east Pacific | 22.75°N 158°W | 56** 102** | 0.21 | 90-130 | Hense and Beckmann, 2008 |
| | | | Sub-tropic region at northeast of Atlantic | 20-35°N 5-30°S | 59 | 0.31 | 80-110 | Perez et al., 2006 |
| | 10-43°E | 19* | | | | | | |
| | Temperate zone | The Sargasso Sea | 30-35°N 61°W | --- | 0.25-0.3 | 100 | Varela et al., 1992 | |
| | | North pacific | 45.17°N 136.93°W | 60 | 0.12 | 55-65 | Anderson, 1969 | |
| Polar region | Southern Ocean | 60-62.5°S 54-62.5°W | 50 | 0.62 | 75 | Holm-Hansen and Hewes, 2004 | | |
| Coastal water | Eastern coastal water of Indian Ocean | Bay of Bengal | 21-30°S 111-115°E | --- | 0.4-0.9 | 85-110 | Hanson et al., 2007 | |
| | | | 21-43°N 88°E | --- | 0.1-0.2 | 65-100 | Murty et al., 2000 | |
| | 11.5°N 81-92°E | 50-100 | | | | | | |
| | The East China Sea | 24.5-26.5°N 120-123.5°E | --- | 0.5-0.8 | 30-50 | Gong et al., 2000 | | |
| | South of Yellow Sea | | 32.7-37°N 119-122.5°E | --- | >2 | 10-20 | Fu et al., 2009 | |
| | | | 122.5-124°E | | <0.5 | 30 | | |
| | English Sea | 49°N 6°W | 5 | 26 | 30 | Sharples et al., 2001 | | |
| | Gulf of Finland | 59.7°N 23.6°E | 5-6 | 1.6-2.5 | 30-35 | Pefros-Alio et al., 1999 | | |
| The Great Wall Bay and is adjacent sea areas at Antarctic | 62°12'-62°14'S 58°56'-58°58'W | --- | 4.1-7.8* | 5-10 | Li. 2004 | | | |

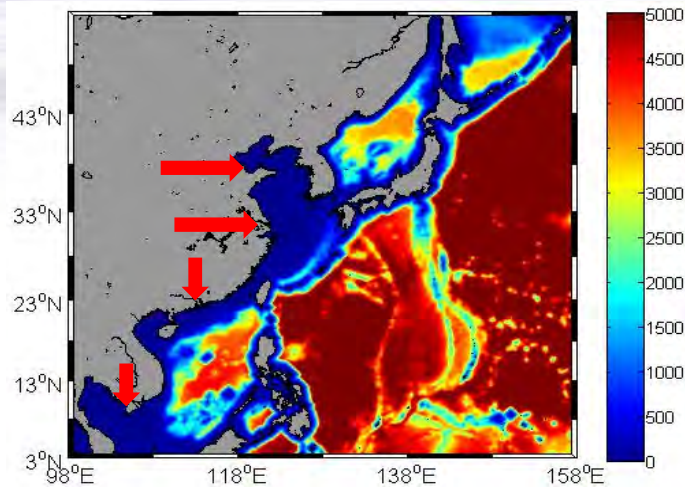
---: lack of data; * integrate concentration value at SCML; **Euler Method(56m) and Lagrange Method (102m).

Gong 2012.



Model Configuration

Physical Model: ROMS



➤ Model Grid Rectangle
Orthogonality

➤ Topography GEBCO 0.5'×0.5'

➤ Establishment

Region : 98°E ~ 158°E , 3°N ~ 52°N ;

Resolution: 1/12° × 1/12° × 22sigma levels;

Open Boundary : South, east and north

| | Yellow River | | Chang Jiang | | Zhu Jiang | | Mekong River | |
|----|--------------|--------|-------------|--------|-----------|--------|--------------|--------|
| | Temp | runoff | Temp | runoff | Temp | runoff | Temp | runoff |
| 1 | 1.1 | 2700 | 6.8 | 9800 | 19 | 4150 | 26 | 7040 |
| 2 | 2.2 | 2000 | 5.4 | 11626 | 19 | 4050 | 26 | 4190 |
| 3 | 6.9 | 6000 | 7.3 | 18201 | 20 | 4100 | 27 | 3020 |
| 4 | 13.6 | 3300 | 11.7 | 16638 | 23 | 6650 | 29 | 2680 |
| 5 | 19.3 | 2600 | 17.9 | 19601 | 25 | 15750 | 30 | 3690 |
| 6 | 23.8 | 2200 | 23.1 | 30382 | 28 | 16850 | 29 | 10400 |
| 7 | 25.9 | 3500 | 25.1 | 42003 | 29 | 19250 | 29 | 17300 |
| 8 | 26.0 | 5200 | 27.0 | 47603 | 29 | 16900 | 28 | 26000 |
| 9 | 20.8 | 2100 | 25.2 | 40509 | 28 | 10900 | 29 | 31000 |
| 10 | 15.1 | 2800 | 22.1 | 25902 | 26 | 8400 | 29 | 29900 |
| 11 | 8.9 | 3800 | 17.0 | 15191 | 23 | 6250 | 28 | 20500 |
| 12 | 1.7 | 2000 | 11.3 | 11201 | 20 | 4900 | 27 | 12100 |

➤ Boundary Data

➤ Climatology Data

➤ Forcing Data

➤ Initial Data

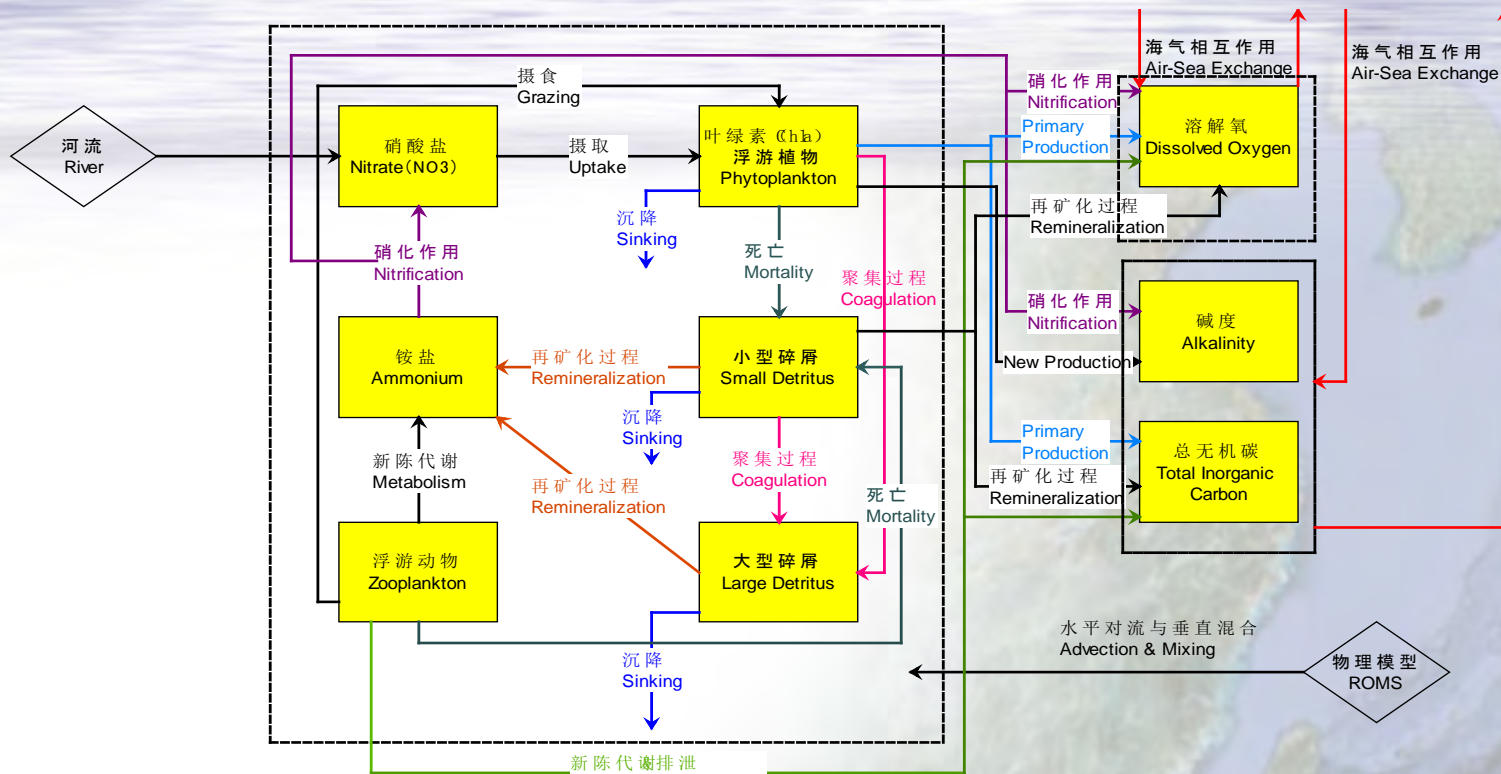
SODA (0.5°×0.5°×40)

COADS and NCEP2
Reanalysis

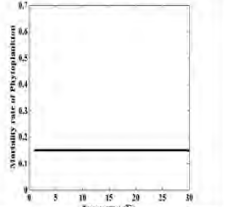
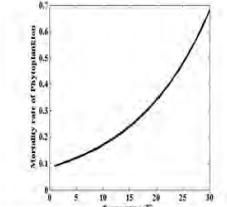
WOA09

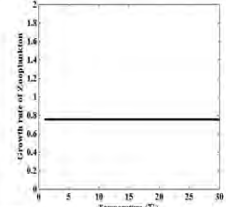
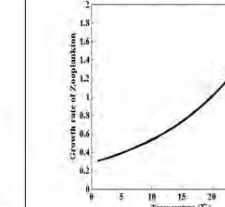


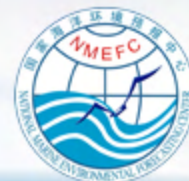
Ecosystem Model Establishment



Model Optimization

| Mortality rate of phytoplankton | |
|---|--|
| Old Model | Modified Model |
| $M_p = \text{Constant}$ | $M_p = M_{or} \cdot \exp(K_{Mor} \cdot T)$ |
| Constant=0.15 | $M_{or}=0.0585$; $K_{Mor}=0.0693$ |
|  |  |

| Growth rate of Zooplankton | |
|---|---|
| Old Model | Modified Model |
| $G_{max} = \text{Constant}$ | $G_{max} = \mu_{20} \cdot q_{10}^{(T-20)/10}$ |
| Constant=0.75 | $\mu_{20}=1$; $q_{10}=1.8840$ |
|  |  |



Initial Conditions for Ecosystem Model

River Input

| Variable | Unit | Initiation and Boundary Filed |
|---------------------|------------------------|--|
| NO3 | mmol N m ⁻³ | WOA09 (1°×1°×24) |
| DO | mmol N m ⁻³ | WOA09 (1°×1°×24) |
| TIC | mmol N m ⁻³ | WOA09 (1°×1°×24) |
| TALK | mmol N m ⁻³ | WOA09 (1°×1°×24) |
| Chlorophyll-a | mg m ⁻³ | SeaWiFS (9km) |
| Phytoplankton | mmol N m ⁻³ | Calculated by Chlorophyll-a (rate: 0.5) |
| Zooplankton | mmol N m ⁻³ | Calculated by Chlorophyll-a (rate: 0.5) |
| Large Detritus(N/C) | mmol N m ⁻³ | Calculated by Phytoplankton (rate: 0.35) Gruber et al., 2006 |
| Small Detritus(N/C) | mmol N m ⁻³ | Calculated by Phytoplankton (rate: 0.35) Gruber et al., 2006 |
| NH4 | mmol N m ⁻³ | Constant as 1 |

| River Month | Yellow River | | Yangtze River | | Pearl River | | Mei Gong River | |
|----------------|--------------|------|---------------|------|-------------|------|----------------|-----|
| | NO3 | NH4 | NO3 | NH4 | NO3 | NH4 | NO3 | NH4 |
| 1 | 22.5 | 48.2 | 40.7 | 10 | 41.4 | 0.7 | 40 | 0.5 |
| 2 | 25.0 | 45.8 | 39.2 | 12.9 | 42.9 | 1.4 | 40 | 1 |
| 3 | 30.0 | 4.2 | 40 | 11.4 | 43.6 | 1.5 | 40 | 1 |
| 4 | 30.0 | 2.1 | 42.1 | 6.4 | 50 | 1.6 | 50 | 1 |
| 5 | 50.12 | 0.75 | 40.7 | 4.3 | 58.6 | 1.52 | 50 | 1 |
| 6 | 24.5 | 3.1 | 42.9 | 4.32 | 57.1 | 1.4 | 50 | 1 |
| 7 | 25.5 | 2.1 | 40 | 6.4 | 59.3 | 0.7 | 50 | 0.5 |
| 8 | 16.56 | 8.9 | 36.4 | 5 | 55.7 | 0.86 | 50 | 0.5 |
| 9 | 19.5 | 0.8 | 35 | 7.1 | 50 | 1.2 | 40 | 1 |
| 10 | 25.0 | 3.5 | 37.9 | 3.6 | 44.3 | 1.1 | 40 | 1 |
| 11 | 25.3 | 37 | 39.2 | 3.6 | 44.3 | 1.2 | 40 | 1 |
| 12 | 24.8 | 15.2 | 42.1 | 6.4 | 42.1 | 1.2 | 40 | 1 |

Zhang, 1996; Duan, 1999; Chen et al., 2010; Zhang et al, 2010



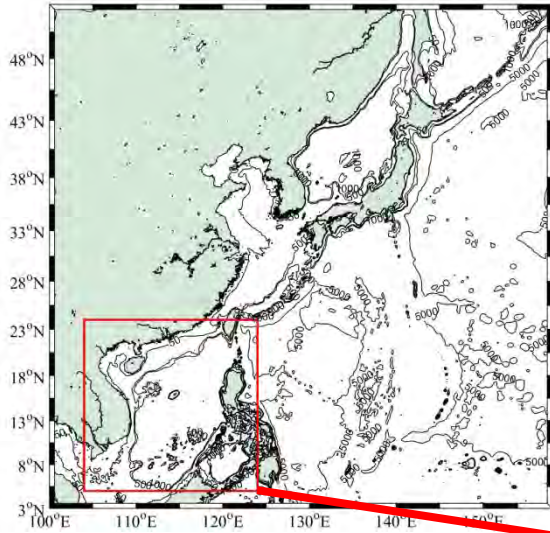
The South China Sea

Model Set up:

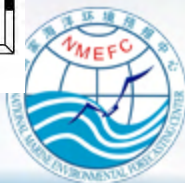
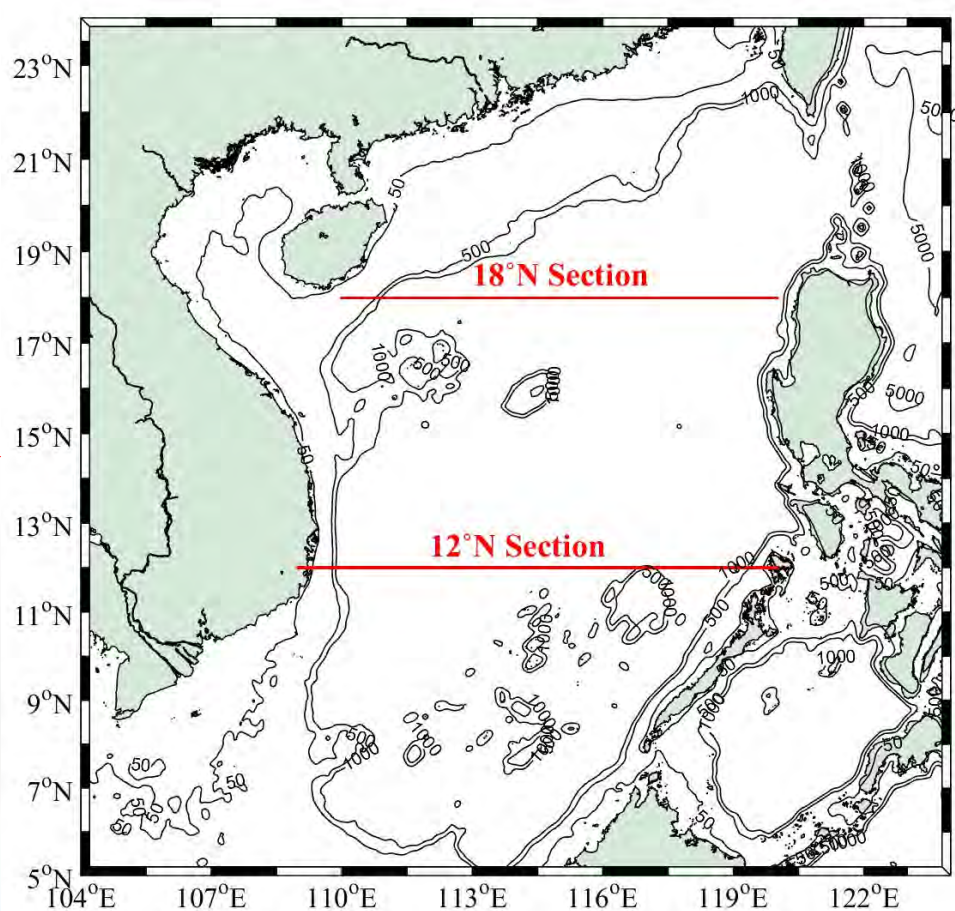
Upper Forcing: NCEP reanalysis data;

Simulation Time: 2001 to 2012;

Output of time resolution: 5 days

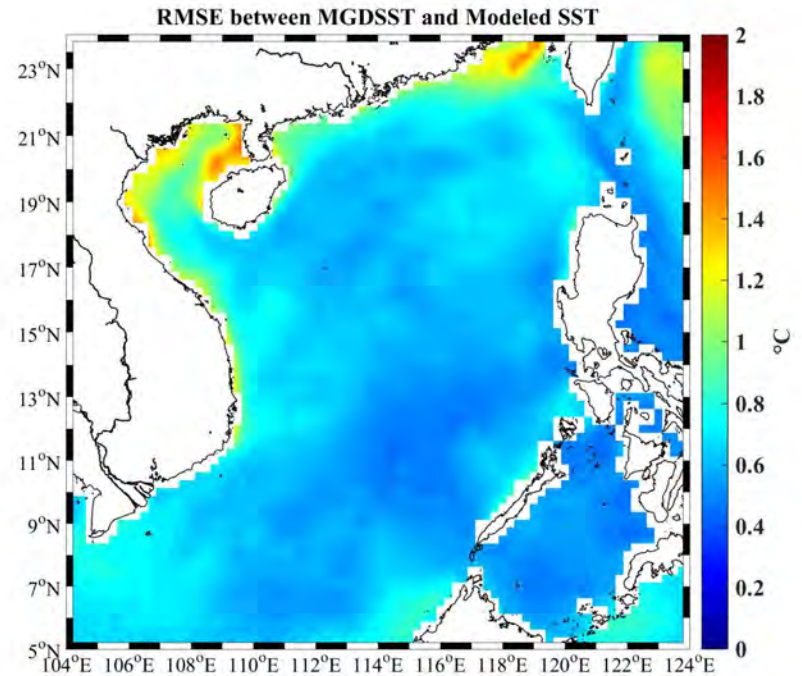
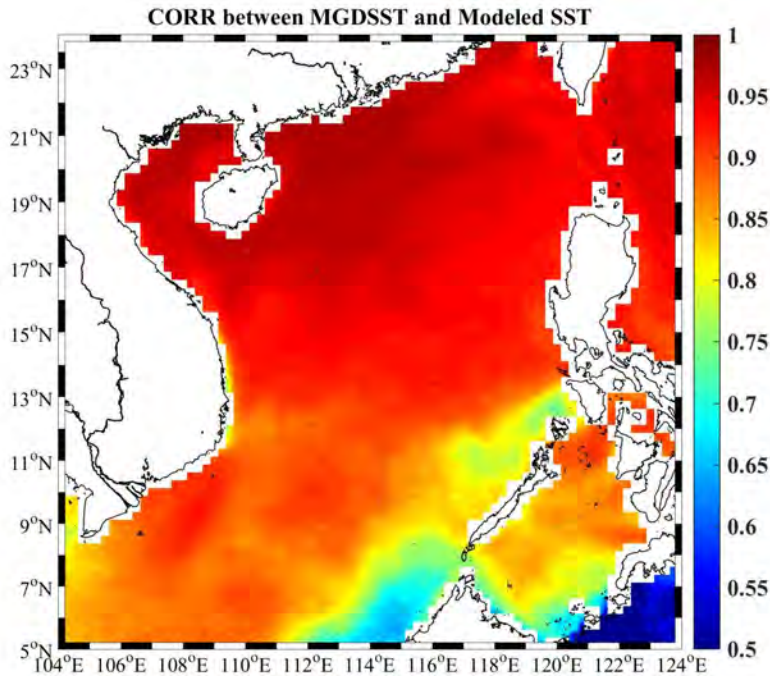


5-24° N; 104-120° E;



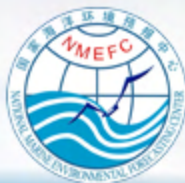
Model Validation

Modeled SST and MGDSST DATA



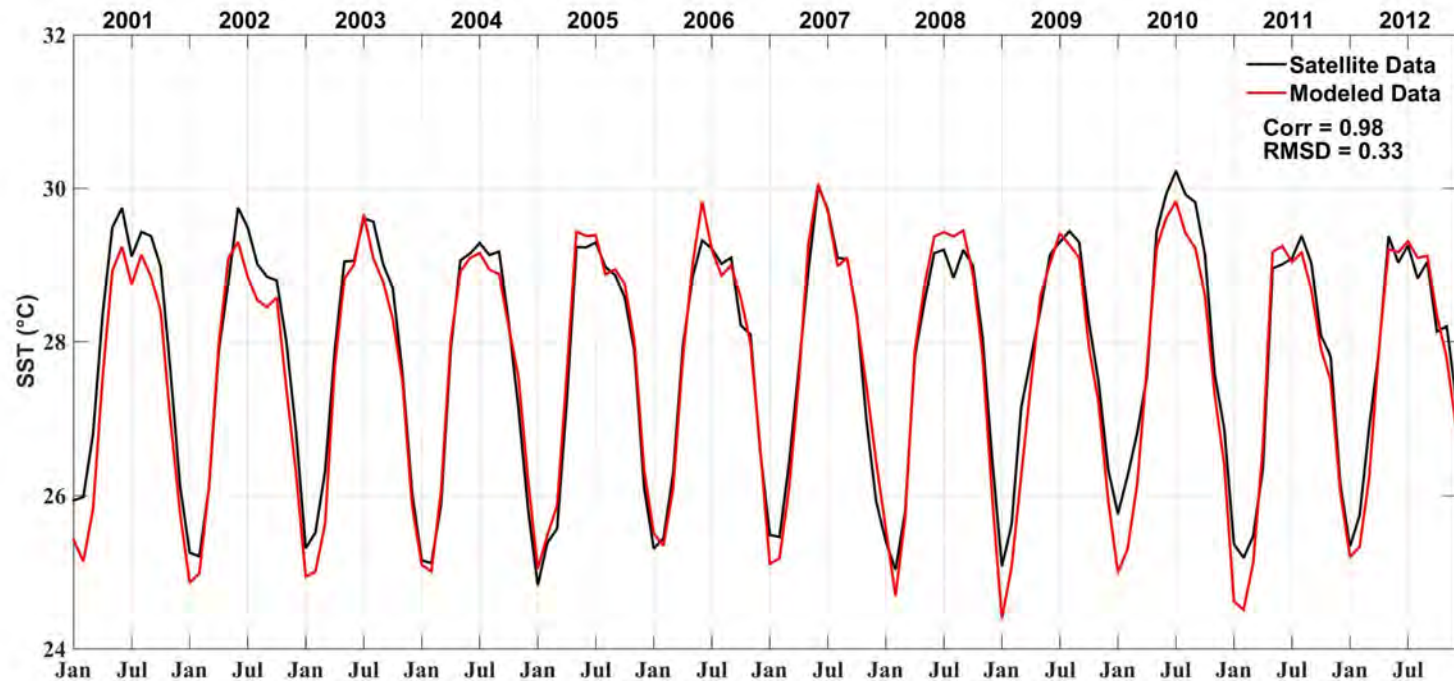
Correlation rate is higher than 0.9 in the north-center of SCS;

RMSE is quite lower in the center of SCS



Model Validation

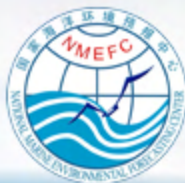
Modeled SST and MGDSST DATA



Black Line: Satellite SST data from MGDSST;

Red Line: Modeled SST data.

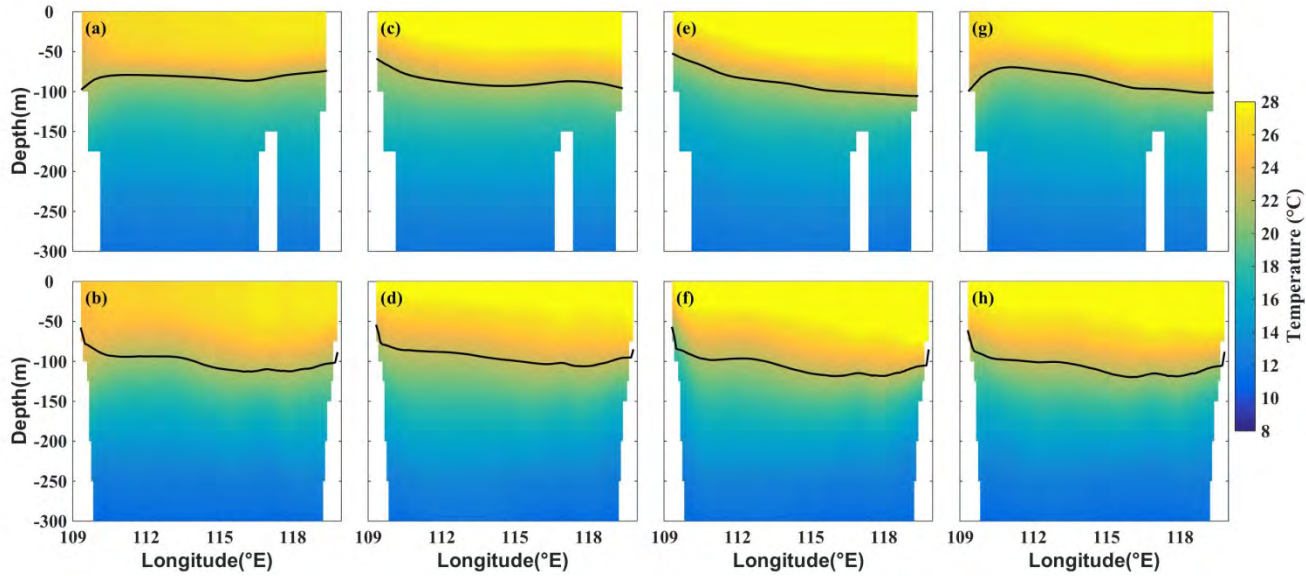
The Correlation rate is 0.98, and RMSD is 0.33, which shows a good performance of physical progress under ROMS model.



Model Validation

---Temperature

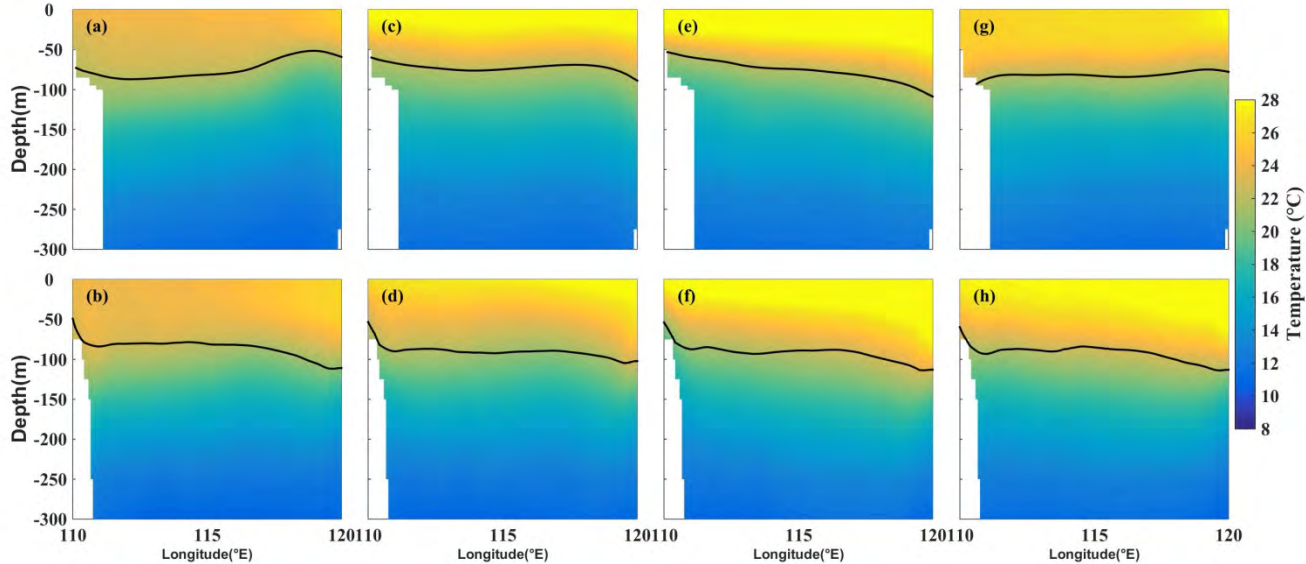
WOA13



12°N剖面

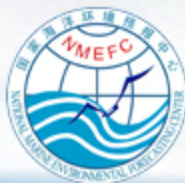
ROMS

WOA13



18°N剖面

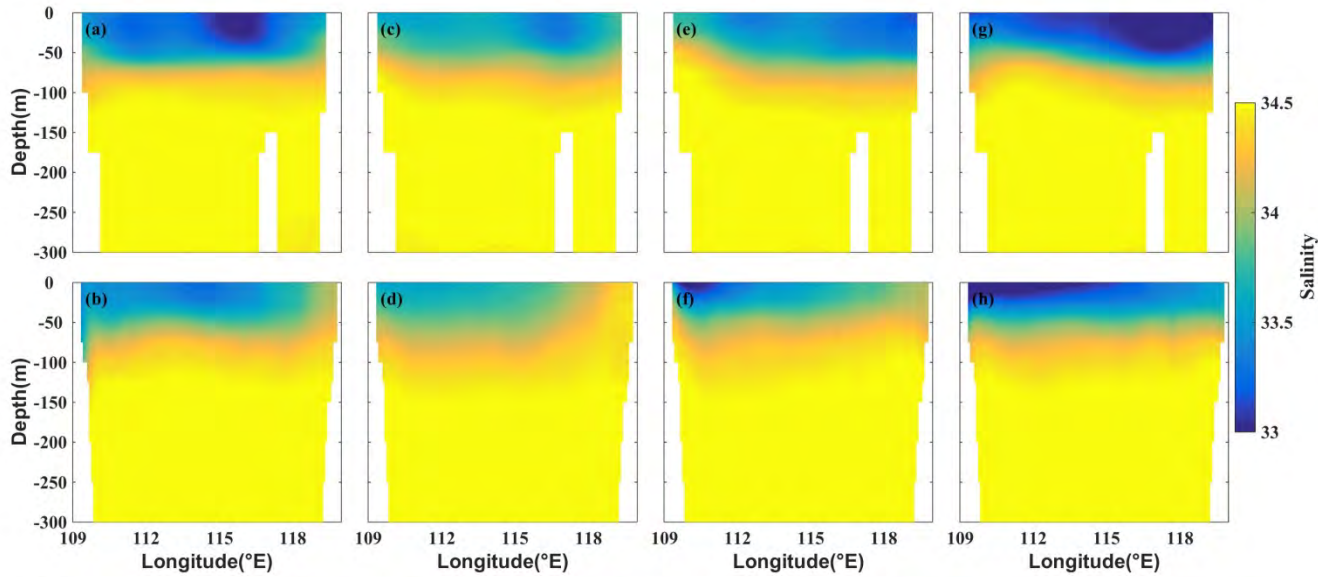
ROMS



Model Validation

---Salinity

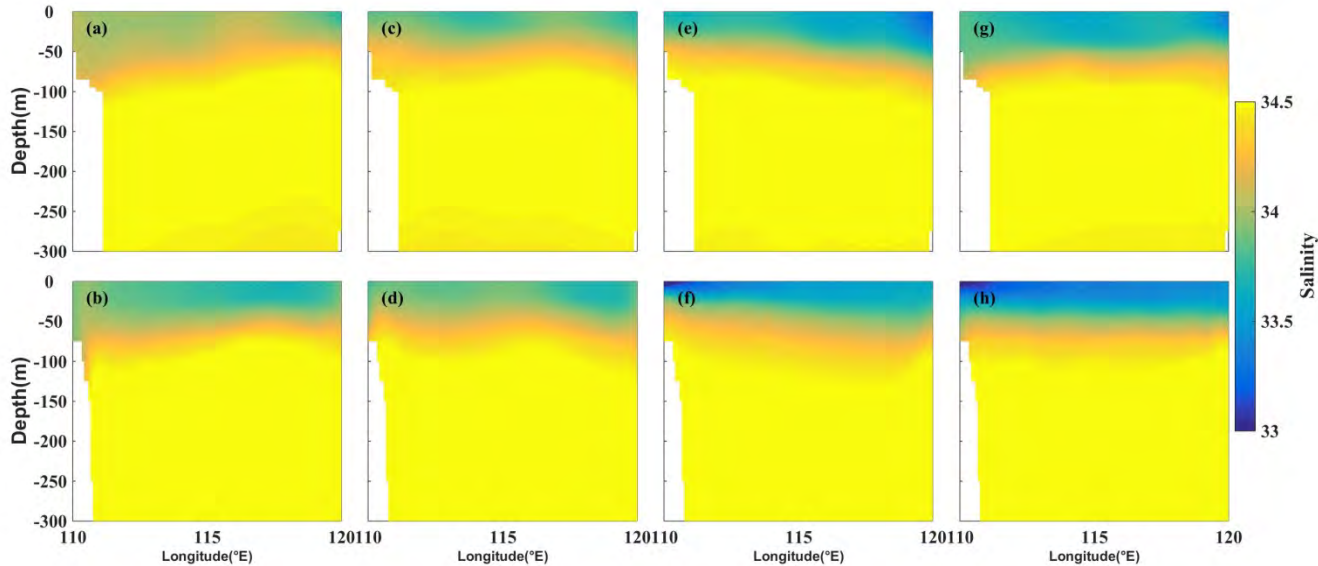
WOA13



12°N剖面

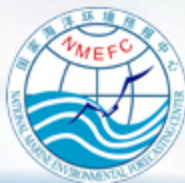
ROMS

WOA13



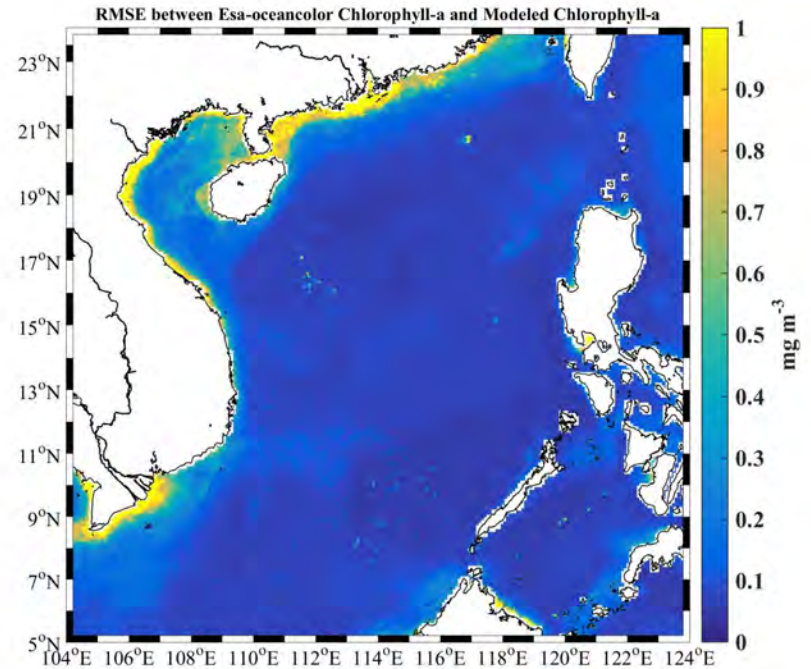
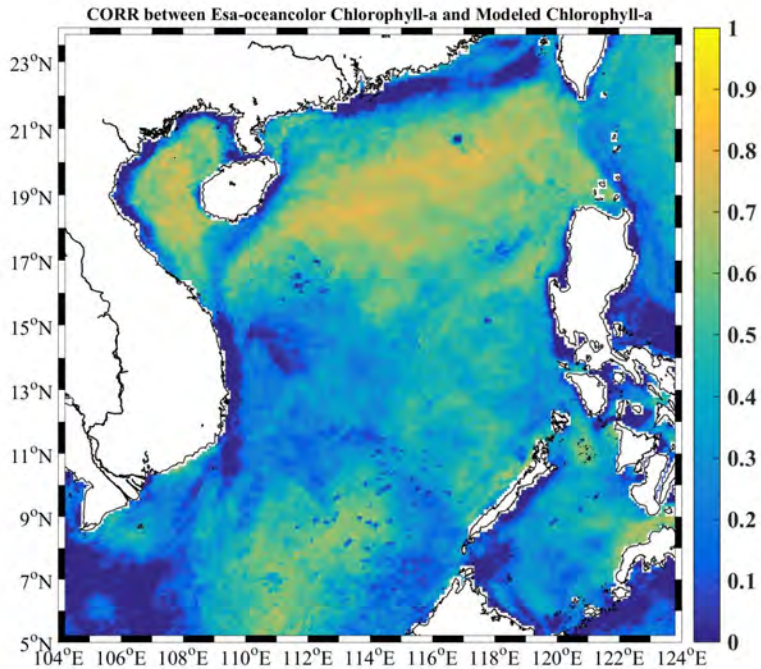
18°N剖面

ROMS



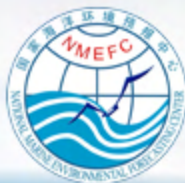
Model Validation

Model Chlorophyll-a and Esa-oceancoulor Chlorophyll-a Data



Correlation rate is higher than 0.9 in the north-center of SCS;
And about 0.7 in the south of SCS

RMSE is quite lower in the center of SCS



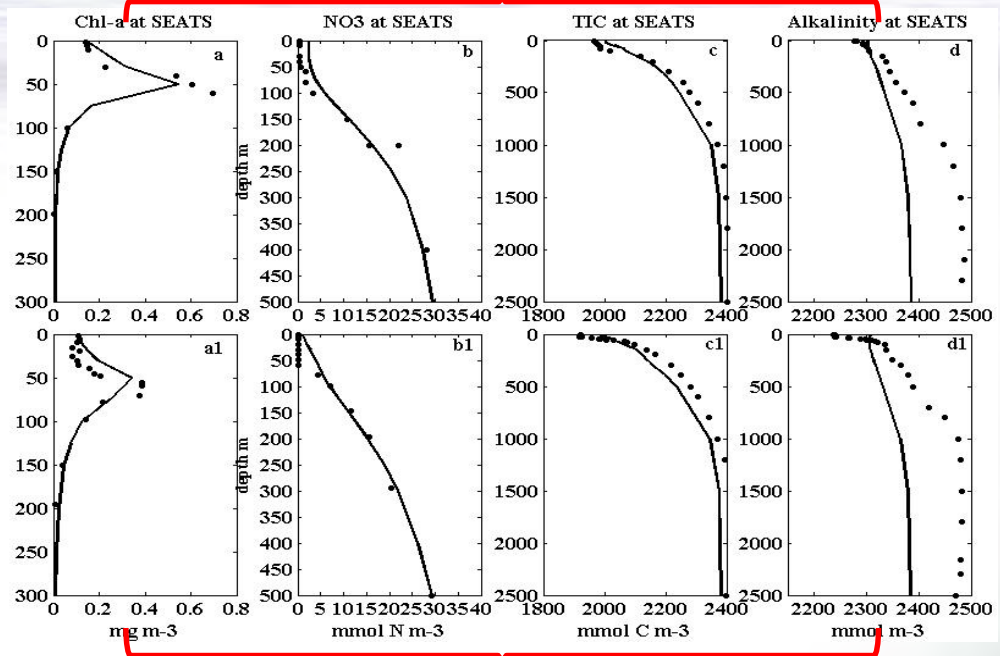
Model Validation

SEATS: 18° N、116° E

Correlation

1

2000.1



Black circle: Obs
 Black line: Model

2000.7

2

1998.9

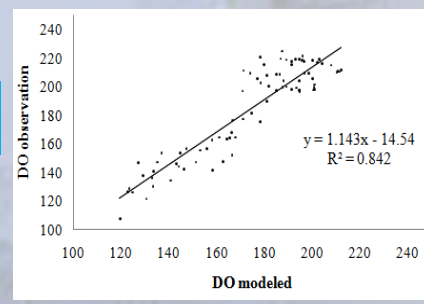
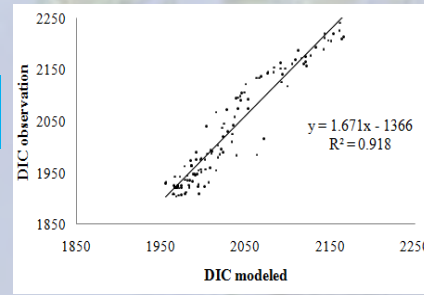
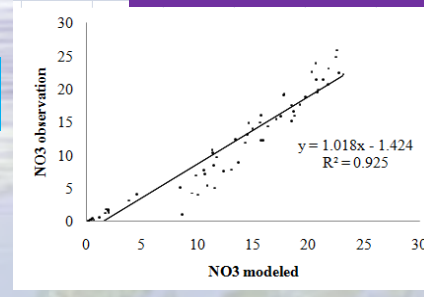
 2000.7

NO₃

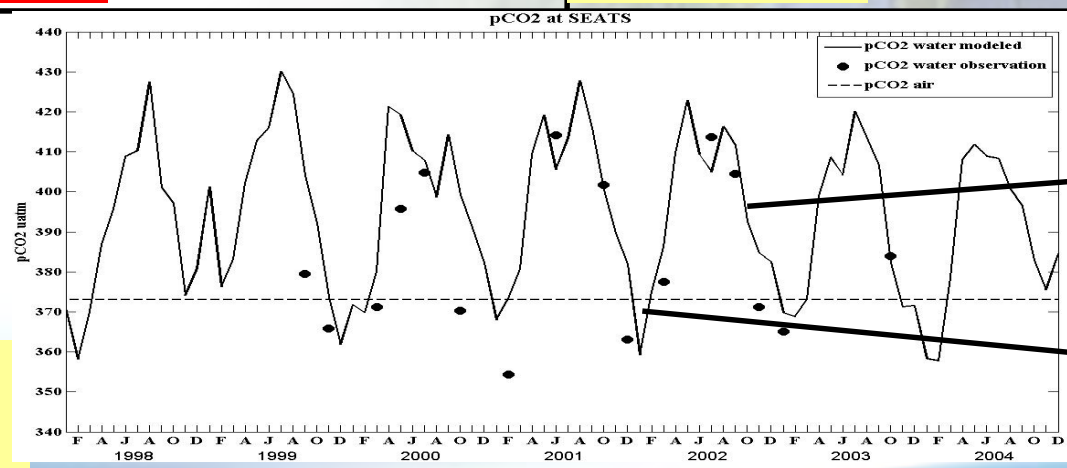
DIC

DO

X: Model
 Y: Obs



3



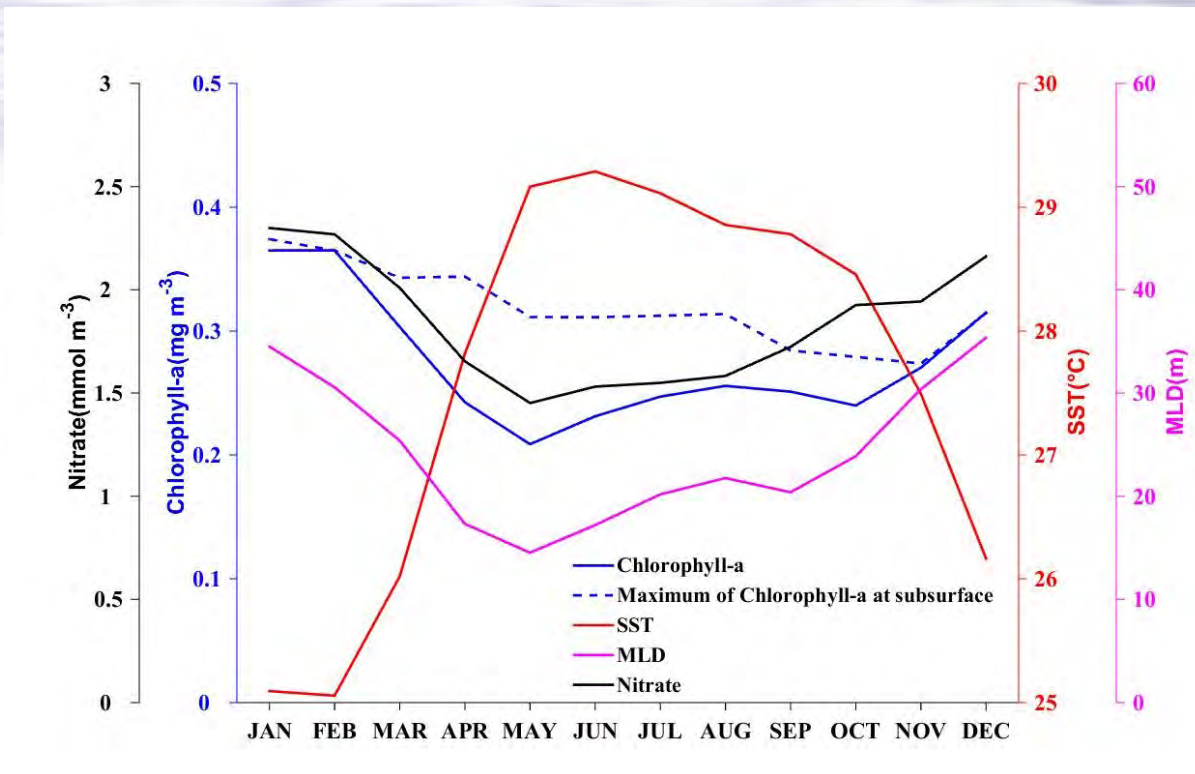
Black circle: Obs from 1999-2003
 Black line: model from 1998-2004
 Black dotted line: air CO₂ 373μatm

3-10月为源

11-2月为汇



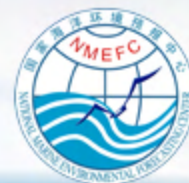
Seasonal Variation of Modeled SST/Chl-a/SCMs/Nitrate/MLD



SST performs a complex changeable characteristic with a small amplitude from 25 to 29.2°C

The surface chlorophyll-a over the entire SCS reveals a strong seasonal cycle, double-peak characteristic, with the highest concentration at winter and a following value at late summer.

The Nitrate concentration reaches the minimum value at spring due to the consumption by the phytoplankton at winter, and then has a supplement at the following months.



Seasonal and Spatial Variation of Modeled Chlorophyll-a

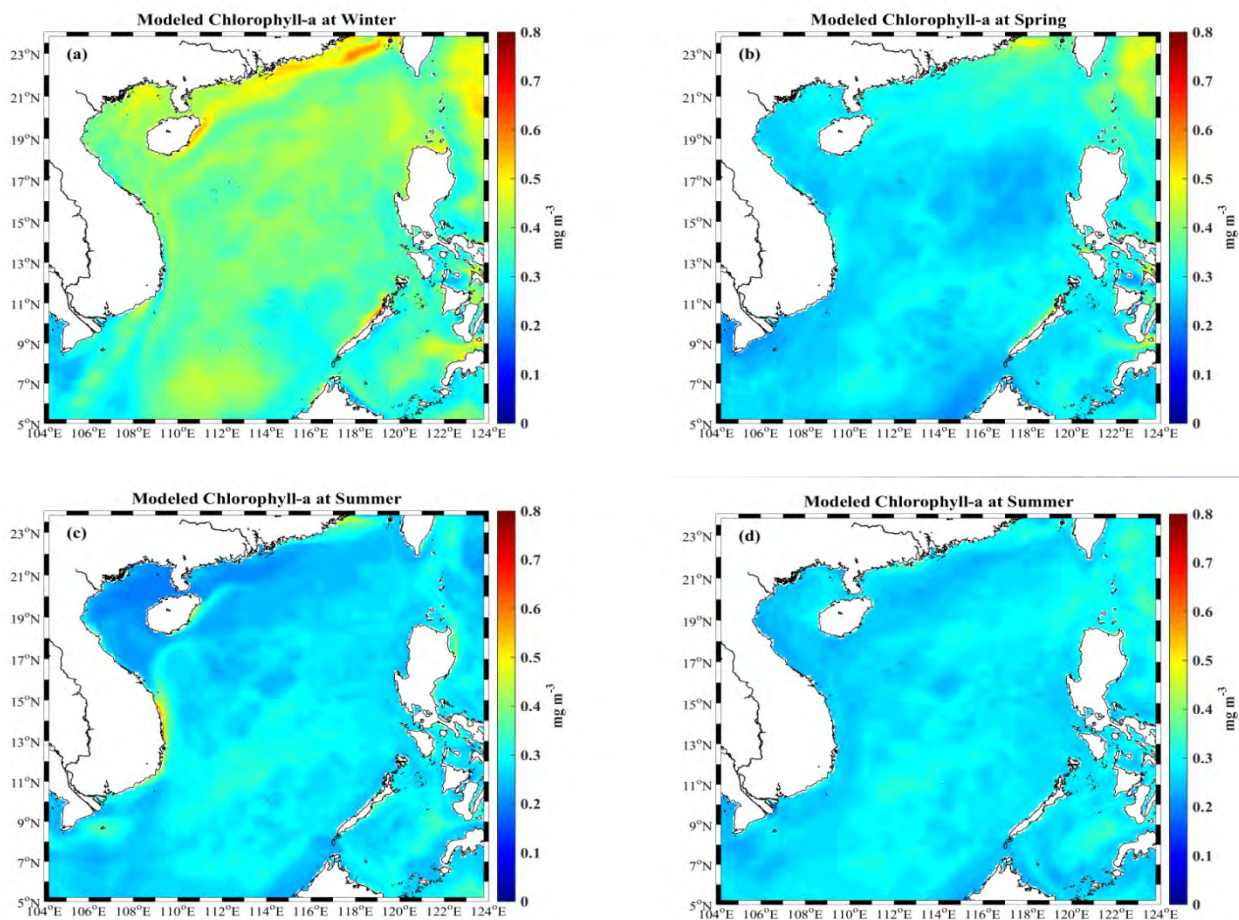


Fig.a : Chlorophyll-a distribution at winter, showing the maximum concentration value during all the year. Due to influence of upwelling under Northeast Monsoon, the chlorophyll-a concentration at west coastal line of Philippine and Palawan Island exists an obvious high value compared with the east coastal line of Vietnam.

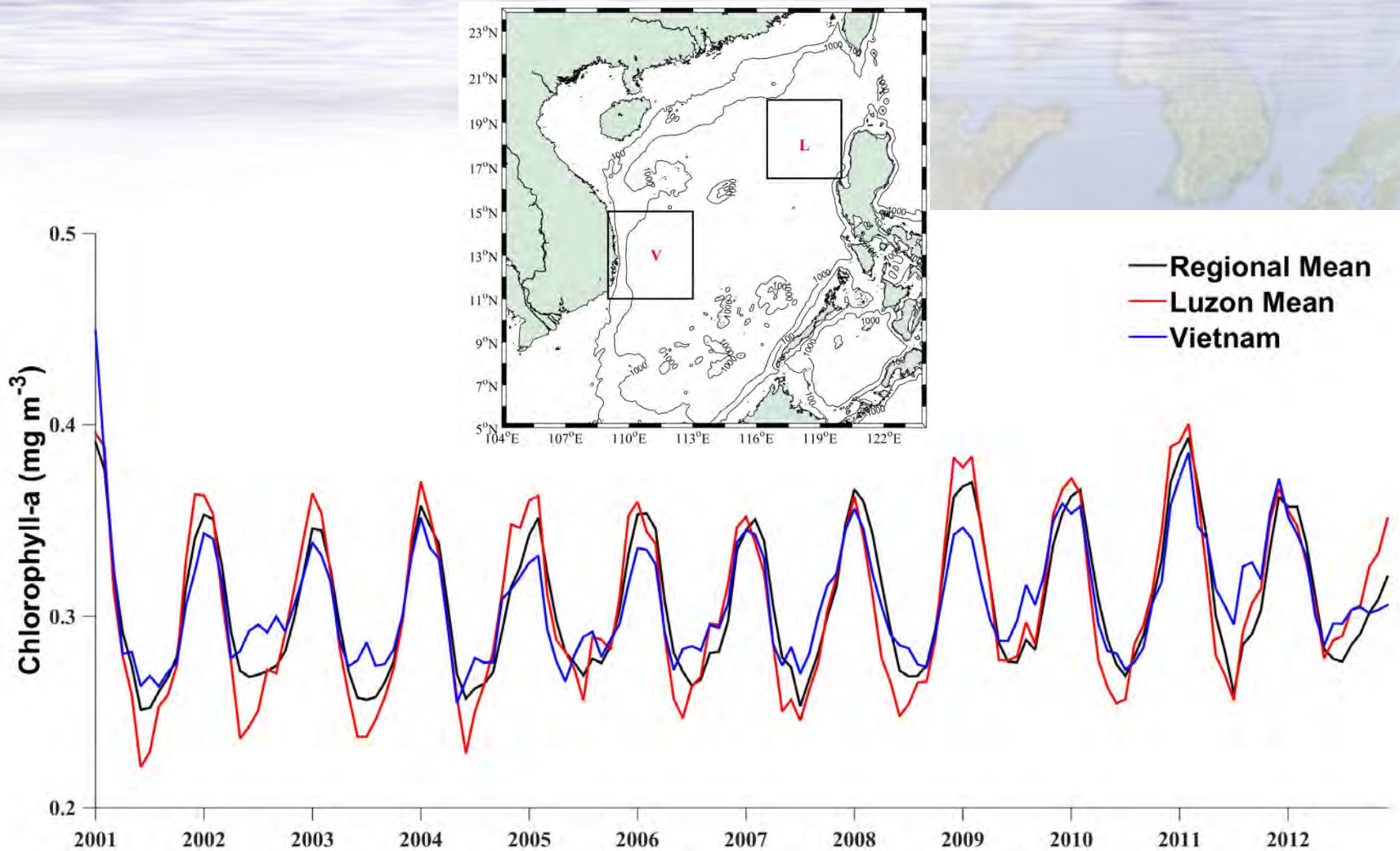
Fig.b: Due to the nutrients absorbed by phytoplankton at winter, the chlorophyll concentration reaches the lowest value in the all year.

Fig.c: In the east of Vietnam, due the upwelling influence, there exists a high concentration of chlorophyll-a, about 0.5 mg m³. For all the region, the chlorophyll-a reaches at a secondary high value followed by winter.

Fig. d, the concentration of chlorophyll-a is lower than that at summer, but higher than at spring.



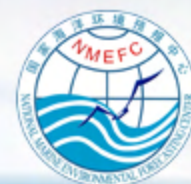
Long-term Variation of Modeled Chlorophyll-a



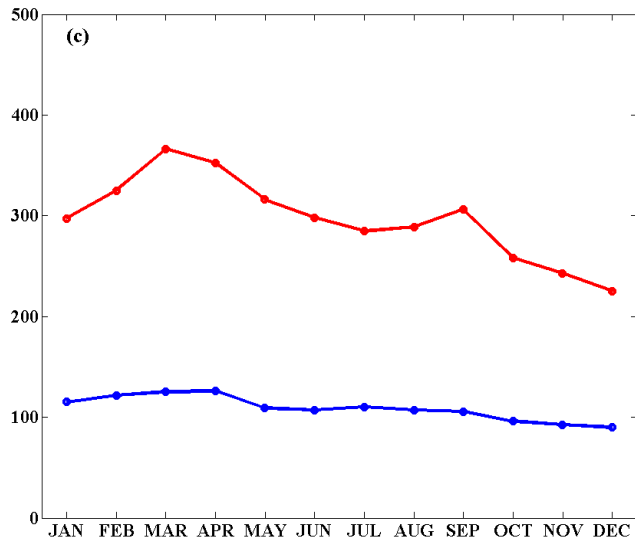
Black line: the regional-mean concentration of Chlorophyll-a;

Red line: the Luzon-mean concentration of Chlorophyll-a, taking an dominant role at winter;

Blue line: the Vietnam-mean concentration of Chlorophyll-a, taking an dominant role at summer.



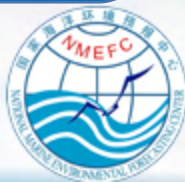
Seasonal Variation of Modeled Primary Production and New Production



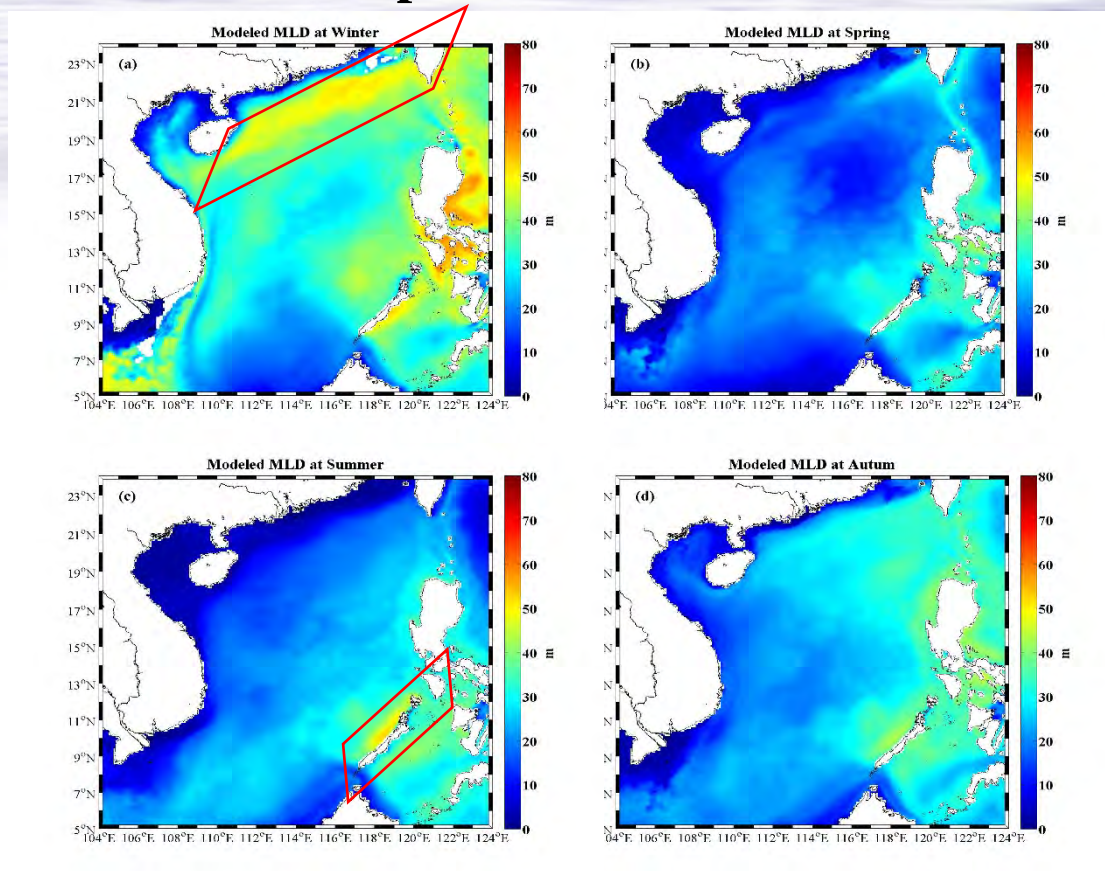
Red Line: Primary Production
Blue Line: New Production

| Annual-mean results in SCS | |
|--|------|
| Primary Production (mgC/m ² /day) | 293 |
| New Production (mgC/m ² /day) | 103 |
| f-ratio (NP/PP) | 0.35 |

f-ratio in SCS is 0.35, similar with results 0.28 ± 0.08 (2001.3), 0.32 ± 0.14 (2002.10) in north of SCS from Chen (2005):



Seasonal and Spatial Variation of Modeled MLD

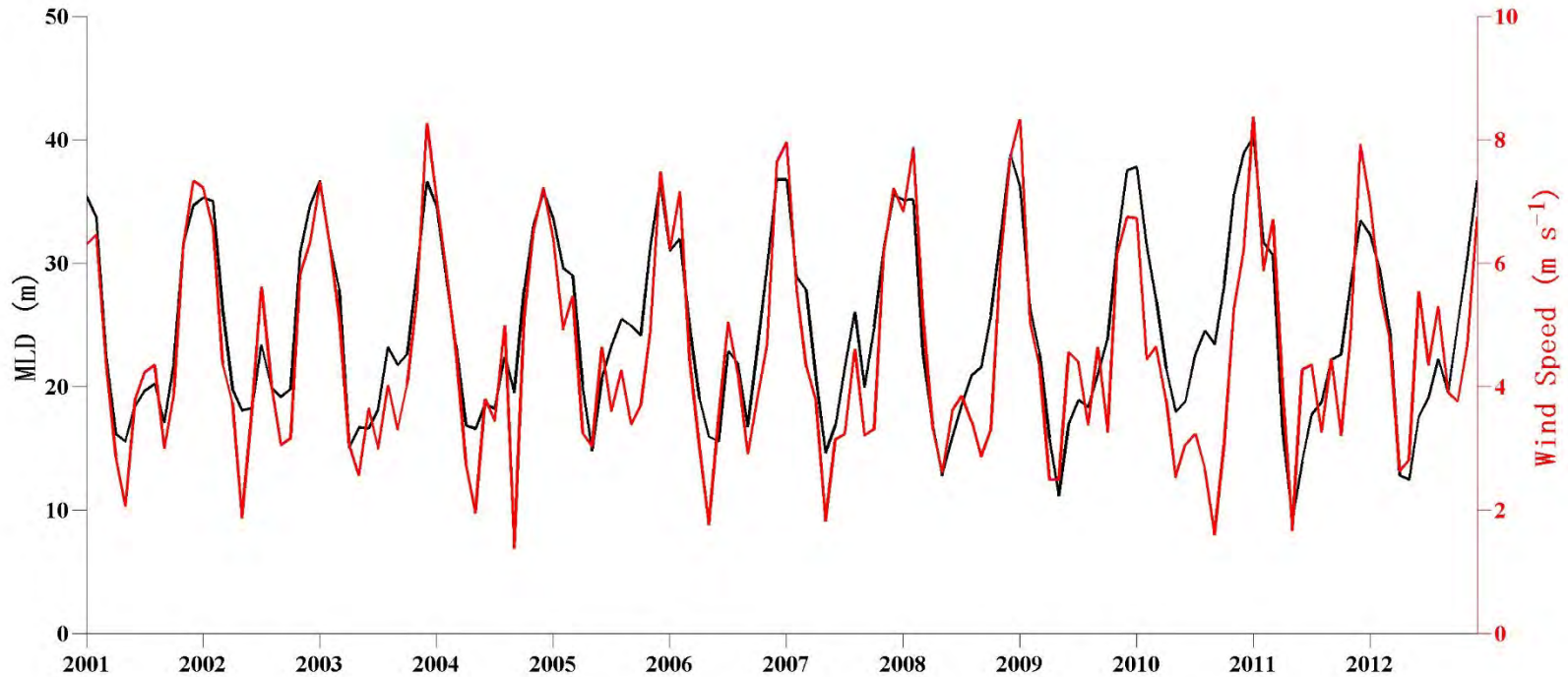


At winter, due to the influence of northeast monsoon, the maximum MLD is located at northwest region of the SCS, about 50m;
At spring, the MLD at SCS region is quite shallow due to the weak monsoon;
At summer, under the effect of southwest monsoon, the maximum MLD is located at the southeast of the SCS, reaches at 55m;
At autumn, due to the monsoon changing and becoming weaker, the MLD is being weaker, but still deeper than that at spring.

Hence, data analysis indicates that monsoon has an obvious impact on the temporal and spatial features of MLD in the SCS through an adjustment of the current field.

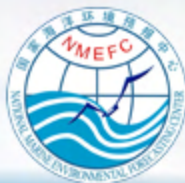


Seasonal Variation of Modeled MLD and Wind

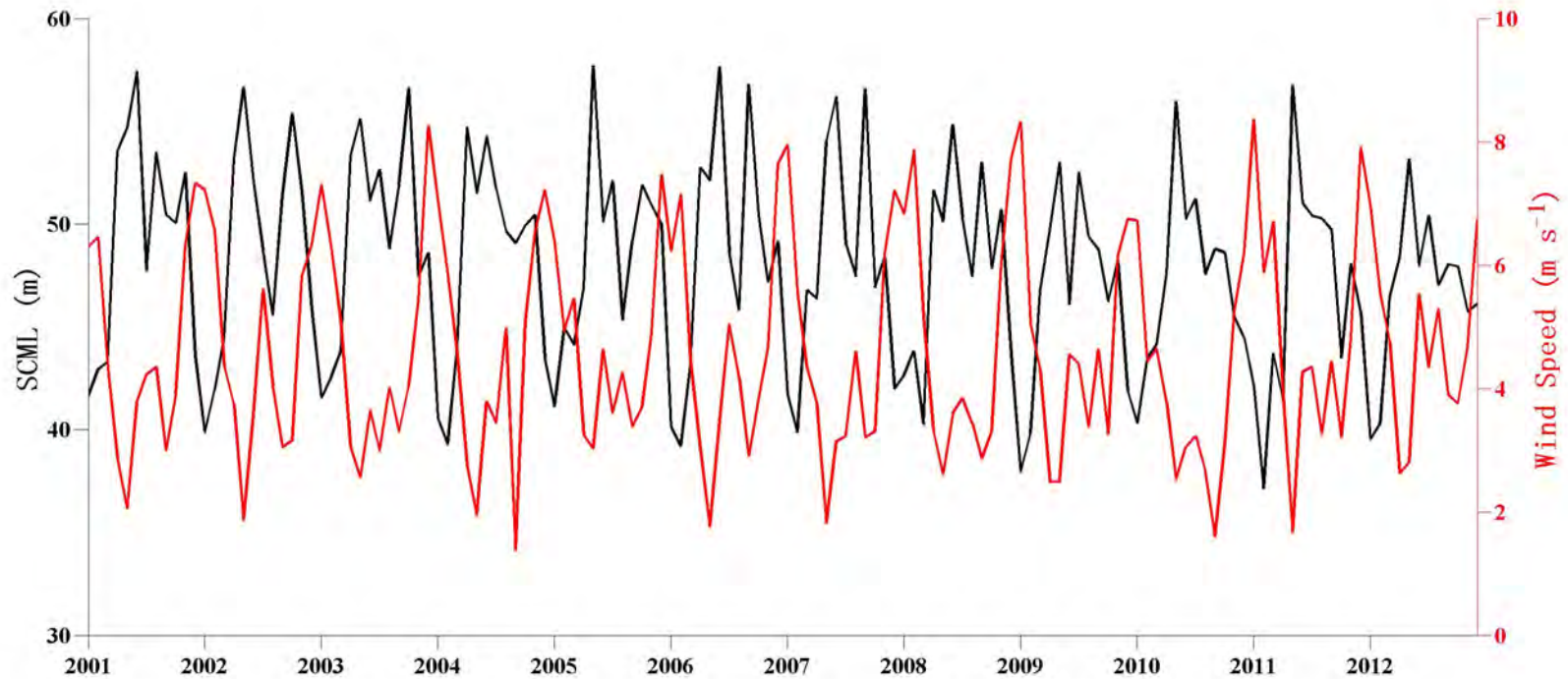


The figure shows the long-term seasonal variation of MLD and wind speed. The black line is MLD, while the red line is wind speed.

The Correlation coefficient between MLD and Wind is 0.87, which shows a positive correlation. The stronger the wind speed, the deeper the MLD.

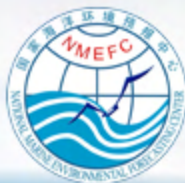


Seasonal and Spatial Variation of Modeled SCML and Wind Speed

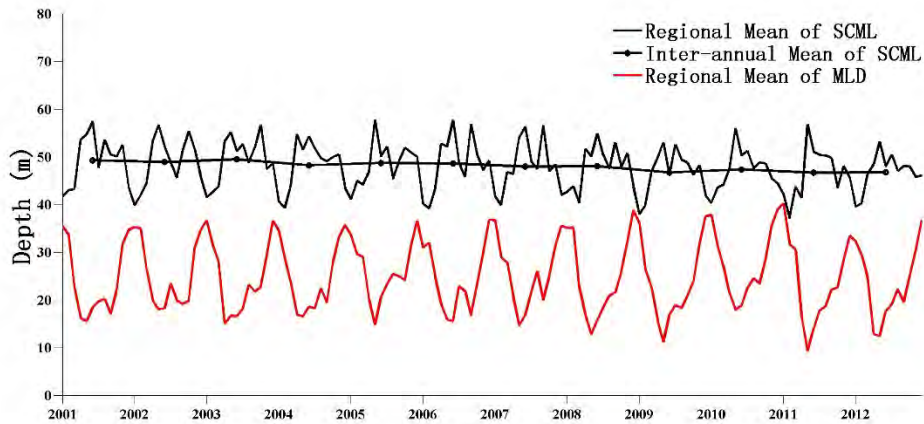


The upper figure shows the long-term distribution of SCML and wind speed. The black line is SCM concentration, while the red line is wind speed.

The Correlation coefficient between SCM and Wind is -0.66, which shows a negative correlation. The stronger the wind speed, the weaker the SCML.



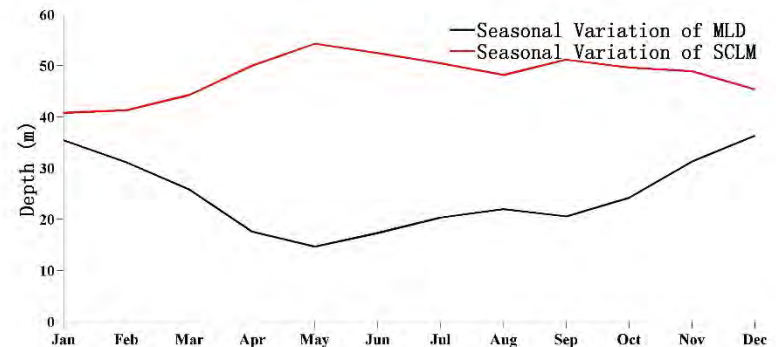
Long-term Variation of Modeled SCML



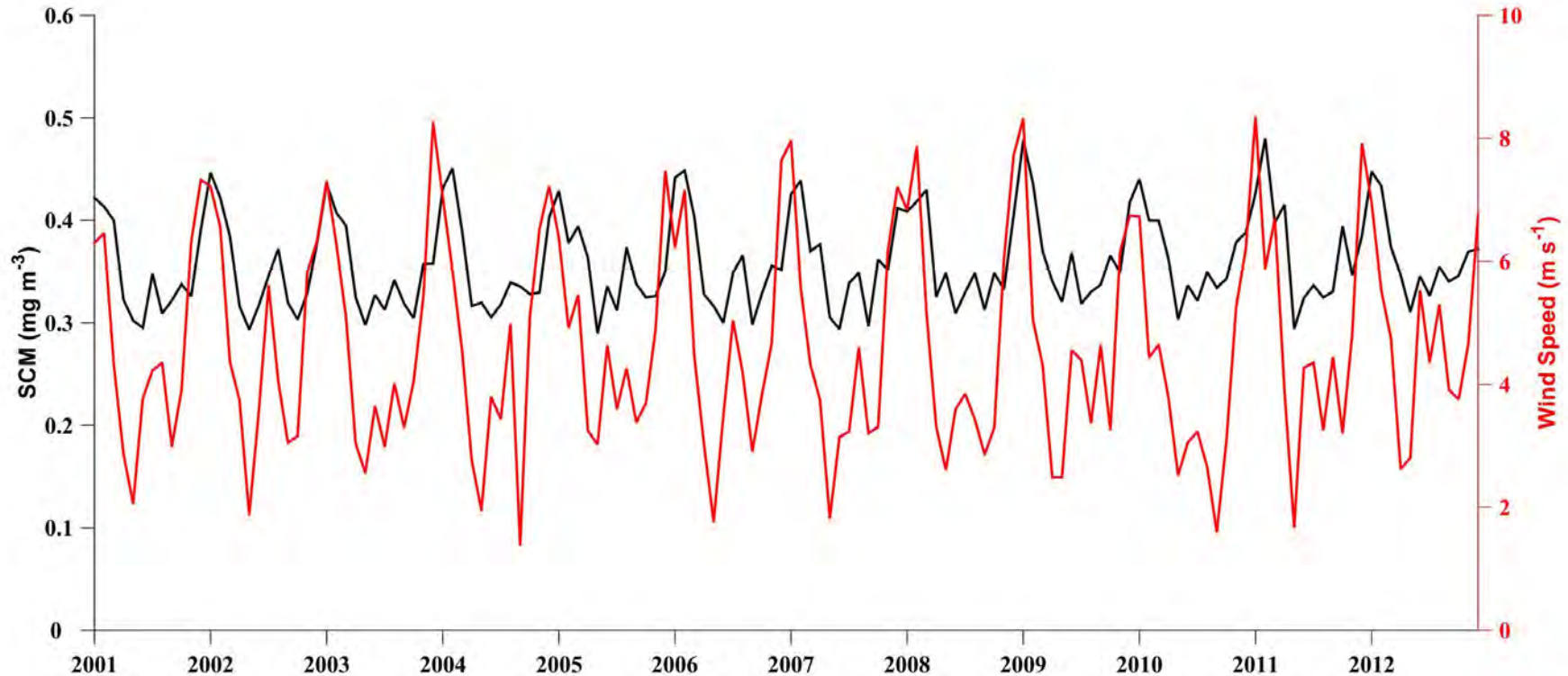
Black line: the regional-mean of SCML;
Circle Black line: inter-annual mean of MLD in the whole region;
Red line: the regional-mean of MLD;
The Correlation coefficient between SCML and MLD is -0.68, which shows a negative correlation.

Black line: the Seasonal Variation of MLD;
Red line: the Seasonal Variation of SCML;

Through the whole year, both of the MLD and SCML performs a double-peak distribution characteristic, one is at May, while the another is at Sep.

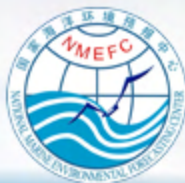


Seasonal and Spatial Variation of Modeled SCM and Wind Speed

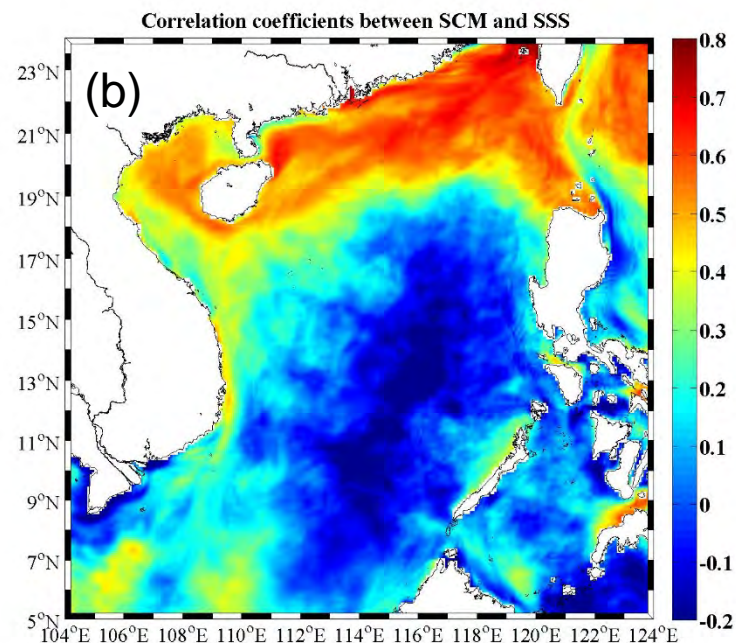
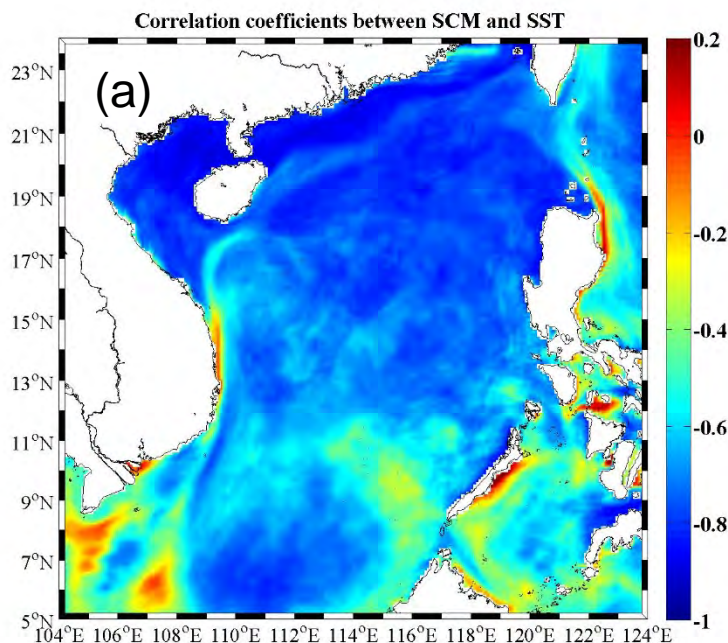


The upper figure shows the long-term distribution of SCM and wind speed. The black line is SCM concentration, while the red line is wind speed.

The Correlation coefficient between SCM and Wind is 0.70, which shows a positive correlation. Stronger wind at winter results in stronger mixing and more nutrients supplied to subsurface, and further resulted in a higher chlorophyll concentration at subsurface.



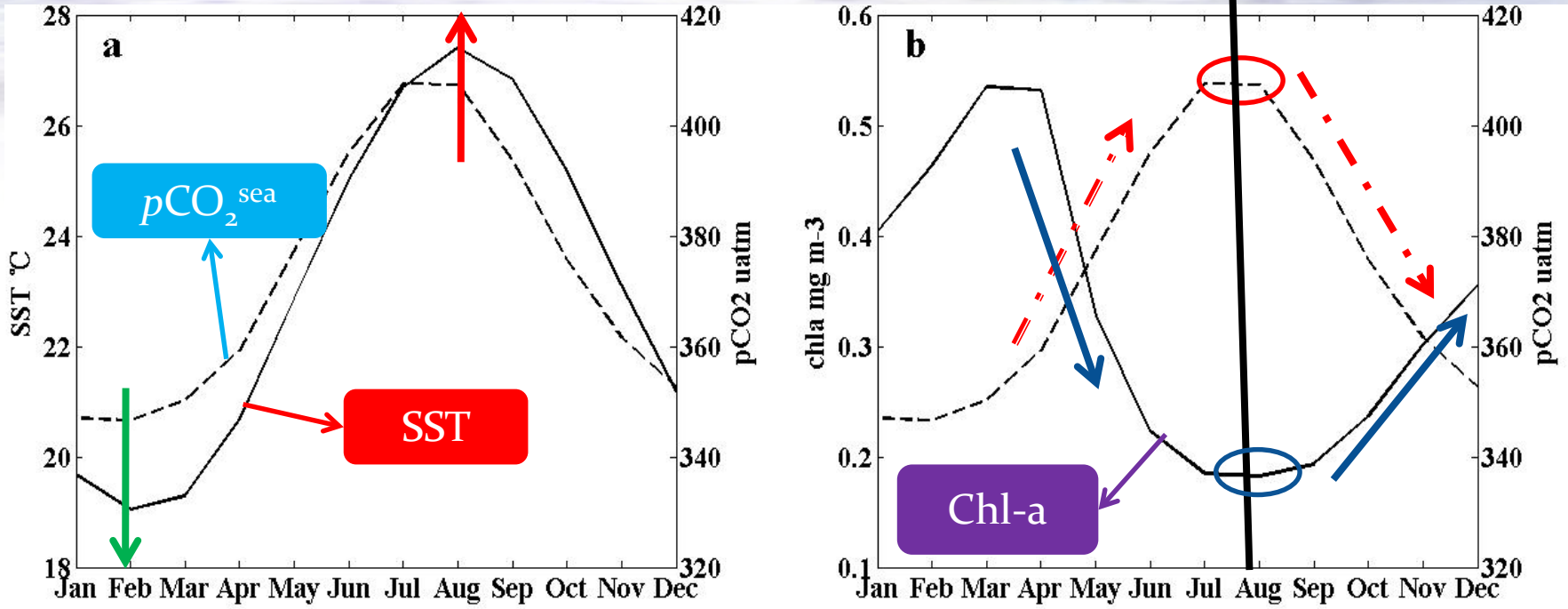
Correlation between Modeled SCM and SSS, SST



The upper figure shows correlation coefficients between SCM and SST (a) and SSS (b). As shown in figure (a), in the SCS region, SCM has a negative relationship with SST, a strongest correlation ratio is found at the northwest of the SCS, reaches at about -0.92, while weaker correlation occurred at the south region of the SCS. However, a positive correlation between SCM and SSS is discovered. The results have good agreements with the results from Liao et al. (2018).

| | temp | salt | Numbers |
|-------------|-------|------|---------|
| Correlation | -0.87 | 0.44 | 144 |

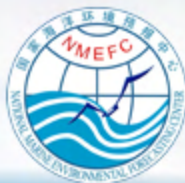
Factors of controlling $p\text{CO}_2^{\text{sea}}$



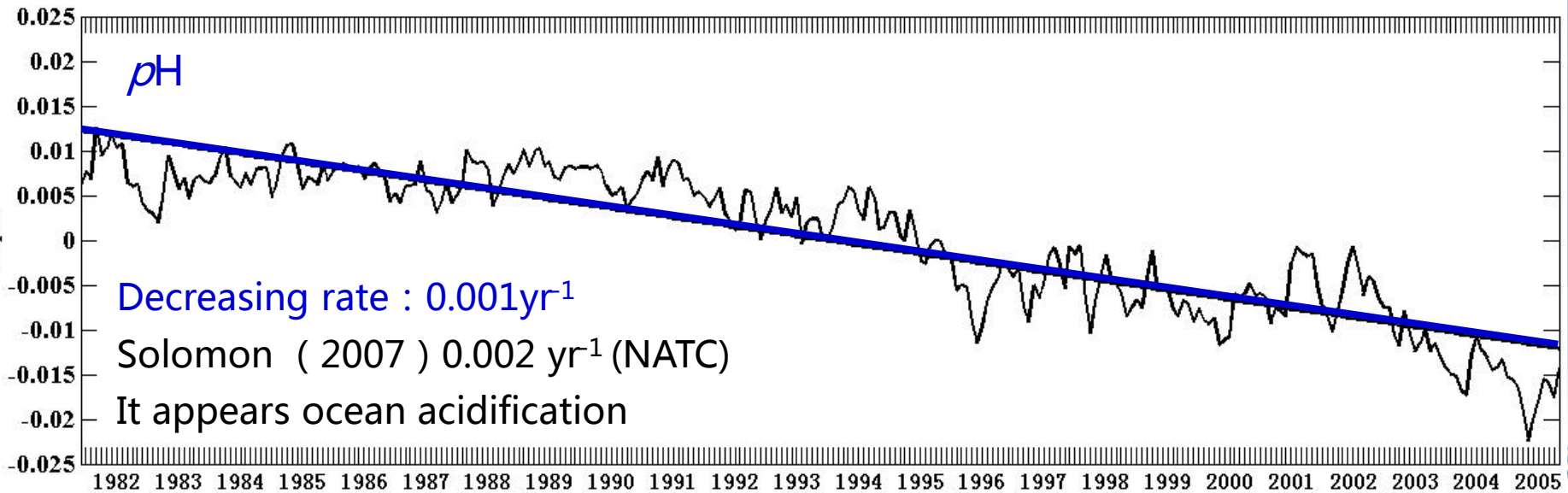
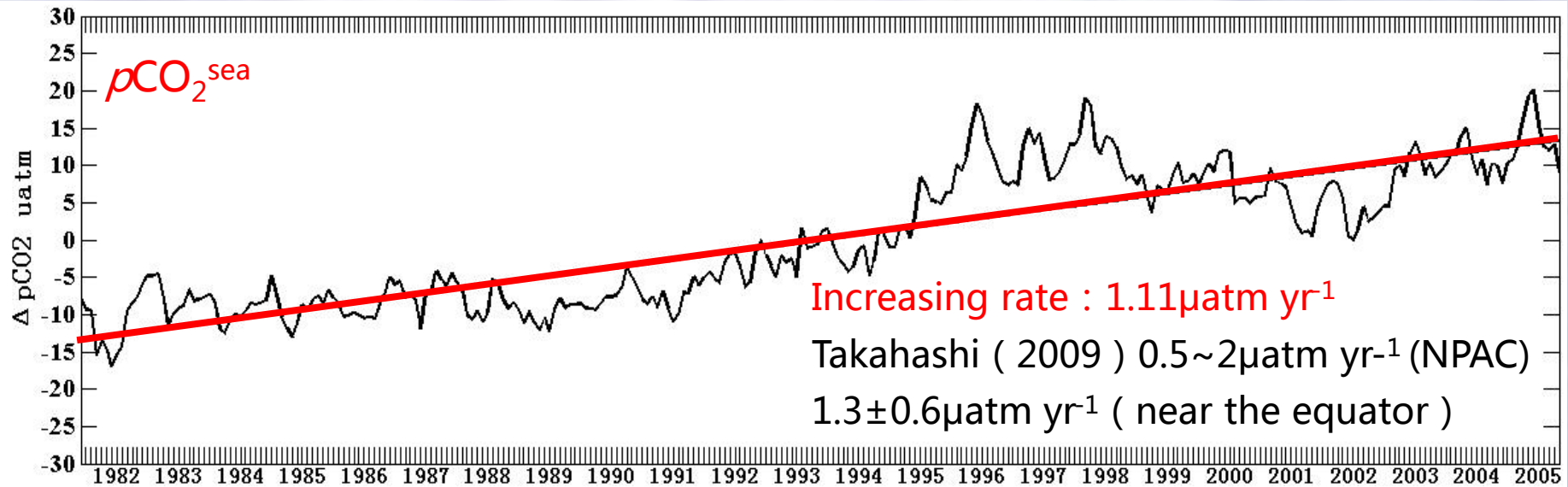
As we can see from the upper picture, the SST varies from 19 to 28, and $p\text{CO}_2$ in seawater changes from 350 to 420 μatm . In figure a, the SST and $p\text{CO}_2$ have a positive relation with each other, reaches the lowest value in February, and gets the highest value in August. While, the $p\text{CO}_2$ has a negative relation with chlorophyll-a, which is shown in figure b. In August, the carbon reaches the highest value, while the chlorophyll has the lowest value.

| | T/B ratio |
|-----|-----------|
| SCS | 1.22 |

According to Takahashi (2002), we found $p\text{CO}_2$ in SCS is mainly controlled by SST, and secondly by biological activity.



Seasonal Variation of pCO₂ and pH



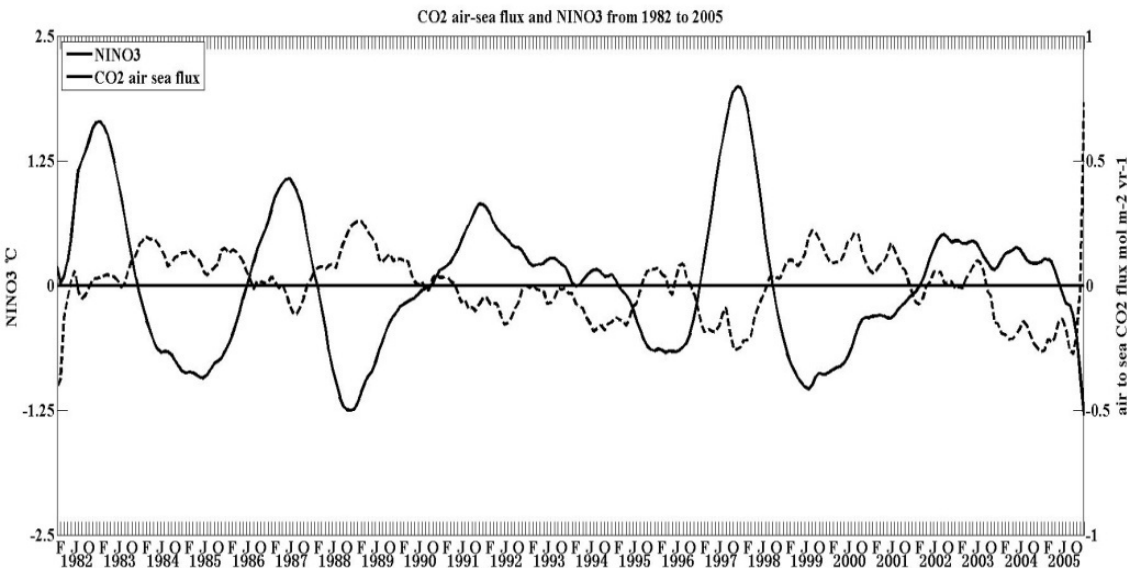
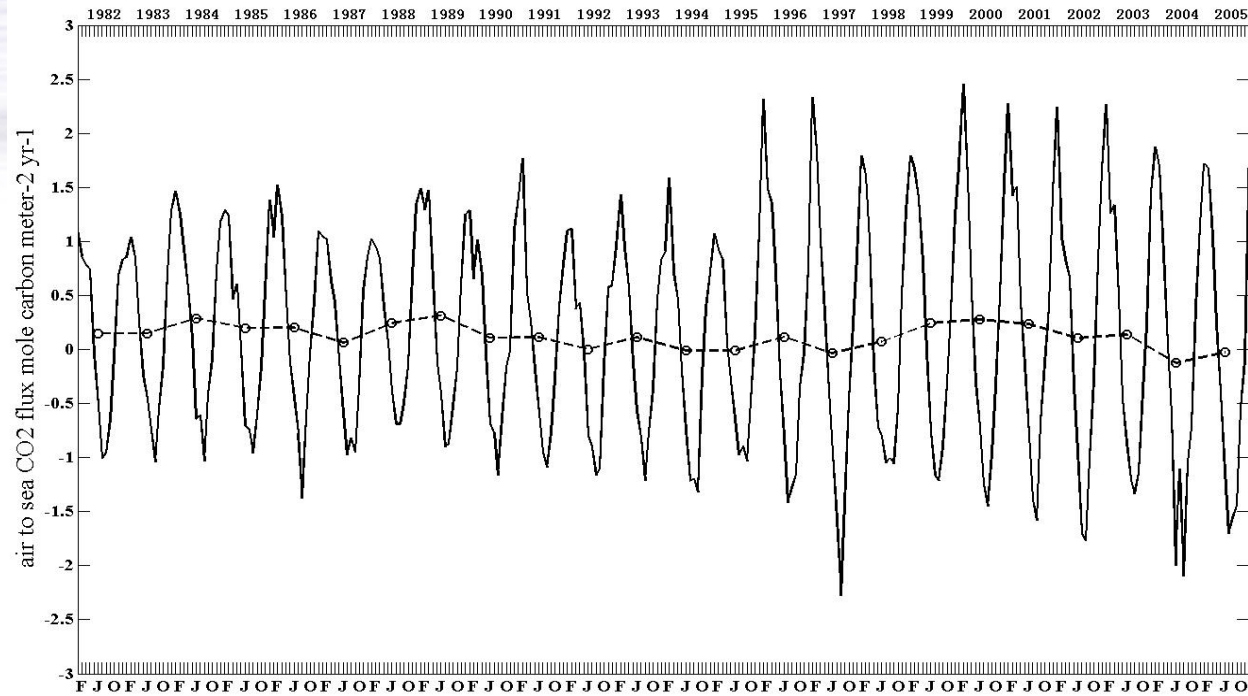
Seasonal and interannual characteristics of air-sea CO₂ flux

Solidline: Monthly mean value;
Circle: interannual mean Value;

Interannual value of Air-sea CO₂ flux varies from -0.13 to 0.31 mol m⁻² yr⁻¹;

Mean value of 24 years: 0.12 mol m⁻² yr⁻¹

Hence, the NWP is a sink of CO₂ to the atmosphere



Solidline: NINO₃ index
Dashes: air-sea CO₂ flux

(1) Positive phase: air-sea CO₂ flux performs a negative value, and reaches the lowest in 1997;

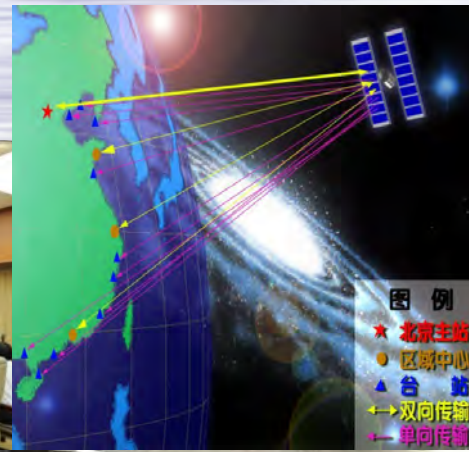
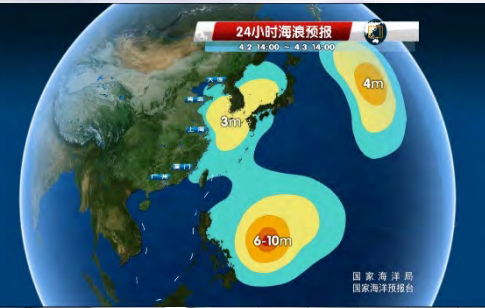
(2) Negative phase: air-sea CO₂ flux performs a positive value;



Conclusion

- On the basis of a regional ocean modeling system (ROMS), a three dimensional physical-biogeochemical model with a resolution of $1/12^\circ \times 1/12^\circ$ is established to investigate the physical variations and ecosystem response in the SCS from 2001 to 2012. The validation results show that the correlation coefficients for modeled SST and Chlorophyll-a are 0.98 and 0.51 and the RMSDs are 0.33 and 0.07 compared with the satellite data of MGDSST and ESA-oceancolor chlorophyll-a data, which means the coupled model has a capability to reproduce the observed seasonal variation features over the same period in the SCS.
- The surface chlorophyll-a over the entire SCS reveals a strong seasonal cycle, double-peak characteristic, with the highest concentration at winter and a following value at late summer.
- The variability of MLD was analyzed by the Empirical Orthogonal Function (EOF). The first mod shows that the variability is same in the whole area of SCS basically with a 42.8% proportion. The second mode shows that the variability is negative-positive dipole-type, and has a positive correlation with a rate of 0.58 when MEI leads 2 month. The third mode performs a positive-negative-positive distribution from south to north, and has a negative correlation with PDO index with a rate of -0.6.
- The MLD and SCML perform an opposite seasonal variation with a same double-peak feature (Spring and Autumn), and the correlation coefficient is -0.68 between each other. The 12 a mean value of SCML is about 48.04m, and MLD is 24.69m.
- The variability of SCML was analyzed by the EOF. The first mod shows that the variability is same in the whole area of SCS basically with a 63.6 % proportion. The largest variability of SCML is located at the west of Philippines, about 116°E and 15°N . The second mode shows that the variability is dipole-type, with a largest negative variability center at the west of Luzon strait, which probably resulted by the Kuroshio intrusion. The positive variability of SCML is at the south of 15°N . The third mode has a strong positive variability center at the east-center of the SCS and the rest regions perform a negative variability.
- The 12 a mean value of subsurface chlorophyll-a maximum is about 0.39mg m^{-3} , and has a positive relation with the wind. The subsurface chlorophyll-a maximum value has a positive correlation with wind and SSS, correlation ratios are 0.70 and 0.44, has a negative correlation with SST, correlation ratio is -0.87.
- The ocean performs an obvious acidification phenomenon, and the air to sea CO_2 flux has a good correlation with ENSO events.





Thanks!

